^{13}C Multiplet Nuclear Magnetic Resonance Relaxation-Derived Ring Puckering and Backbone Dynamics in Proline-Containing Glycine-Based Peptides

Dmitry Mikhailov, Vladimir A. Daragan, and Kevin H. Mayo
Department of Biochemistry, Biomedical Engineering Center, University of Minnesota Health Sciences Center, Minneapolis, Minnesota 55455 USA

ABSTRACT $^{13}CH_2$-multiplet nuclear magnetic resonance relaxation studies on proline (P)-containing glycine (G)-based peptides, GP, PG, GPG, PGG, and GPGG, provided numerous dipolar auto- and cross-correlation times for various motional model analyses of backbone and proline-ring bond rotations. Molecular dynamics simulations and bond rotation energy profiles were calculated to assess which motions could contribute most to observed relaxation phenomena. Results indicate that proline restricts backbone Ψ_1, Ψ_2, and ϕ_2 motions by 50% relative to those found for a polyglycine control peptide. Ψ_1 rotations are more restricted in the *trans*-proline isomer state than in the *cis* form. A two-state jump model best approximates proline ring puckering which in water could occur either by the C_γ endo-exo or by the C2 interconversion mechanism. The temperature dependence (5° to 75°C) of C_β, and C_γ, and C_δ angular changes is rather flat, suggesting a near zero enthalpic contribution to the ring puckering process. In lower dielectric solvents, dimethylsulfoxide and methanol, which may mimic the hydrophobic environment within a protein, the endo-exo mechanism is preferred.

INTRODUCTION

Recently, nuclear magnetic resonance (NMR) relaxation studies of protein backbone/side-chain motional dynamics could be undertaken for several reasons, including NMR instrumentational and methodological advances, development of genetic cloning techniques and peptide synthesis for ^{13}C- and ^{15}N-enriched samples, and increased computational power for model analyses. Most motional dynamics studies are focused on the use of ^{13}CH and ^{15}NH bond rotational auto-correlation times derived from proton-decoupled NMR relaxation spectra (see Clore and Gronenborn, 1993). Novel two-dimensional NMR methods have been developed to derive considerable information from a few experiments and to resolve more and more resonances for which numbers increase with the size of the biopolymer. However, by doing this, unique motional information is lost by not performing multiplet relaxation (proton-coupled NMR spectra) studies from which dipolar cross-correlation spectral densities can be derived. Relative to auto-correlation functions, cross-correlation spectral densities are more sensitive to rotational anisotropy, provide additional internal motional information on correlated rotations of different internuclear vectors in methylene and methyl groups (Werbelow and Grant, 1977; Grant et al., 1991; Daragan and Mayo, 1993a, b), and allow better discrimination among various rotational models. The trade-off here is that higher dimensional NMR experiments are less effective for multiplet relaxation studies because of significant decreases in signal to noise and potential overlap of multiplet resonances. For accurate measurements, therefore, one is currently limited to perform conventional one-dimensional NMR multiplet relaxation experiments.

The study of short peptides provides an informational foundation on backbone and side-chain motions in the absence of most steric effects found in folded proteins. Only intraresidue and direct neighbor interresidue steric effects contribute to internal motions in a short peptide. In addition, motional model analyses involving all possible internal rotations and long time scale molecular dynamics simulations can be performed relatively simply. Such analyses allow one to discriminate among various rotational models, to choose the best one that can describe specific internal bond rotations, and to apply refined motional models to the analysis of larger peptide and protein dynamics.

Proline, an imino acid, is known to restrict conformational space and, via *cis-trans* isomerization of the peptide bond, to limit the rate of protein folding (Jaenicke, 1991). Observation of significant differences in ^{13}C relaxation parameters for pyrrolidine ring carbons (London, 1978, and references therein) had stimulated earlier NMR relaxation studies of proline incorporated into various peptides. Inasmuch as, for short peptides, $\{^1H\}$-^{13}C nuclear Overhauser effects reach a maximal value and spin-spin relaxation times (T_2) equal spin-lattice relaxation times (T_1), nuclear Overhauser effects and T_2 values provide no additional motional information. With only ^{13}C T_1 relaxation data, one can determine four bond rotational auto-correlation, τ_{CH}, times, one for each of the proline ring CH bonds. This limits the rotational model analysis to determine only four motional parameters. Additional motional parameters, however, can be derived from proton-coupled ^{13}C inversion-recovery experiments that

Received for publication 8 September 1994 and in final form 18 January 1995.

Address reprint requests to Dr. Kevin H. Mayo, Department of Biochemistry, NMR Lab Box 609, University of Minnesota, 420 Delaware St. SE, Minneapolis, MN 55455. Tel.: 612-625-9968; Fax: 612-626-2325; E-mail: I-plei@maroon.tc.umn.edu.

0006-3495/95/04/1540/11 $2.00

yield cross-correlation (τ_{HCH}) times for the three methylene groups of the proline ring (see Theory). Better model discrimination can be had by using seven motional parameters. Moreover, cross-correlation spectral densities are more sensitive to rotational anisotropy and therefore to motional restrictions.

In this paper, auto- and cross-correlation times have been measured for all methylene groups in several proline (P)-containing, glycine (G)-based di-, tri-, and tetrapeptides, i.e., GP, PG, GPG, PGG, and GPGG. Relaxation data have been collected as a function of temperature, at various pH values, and in water, dimethylsulfoxide (DMSO), and methanol. Analysis with various rotational models has indicated that a two-state jump model with diffuse motions within potential wells best accounts for backbone and proline ring puckering motions. Backbone motions about the *trans*-proline bond are more restricted than in the *cis*-isomer state. Experimental results are compared with molecular dynamics simulations done in water.

THEORY

^{13}C auto-[$J_{CH}^*(\omega)$] and cross-[$J_{HCH}(\omega_C)$] correlation spectral densities can be derived from standard proton-coupled ^{13}C inversion-recovery NMR relaxation experiments (Werbelow and Grant, 1977; Grant et al., 1991; Daragan and Mayo, 1993b) by measuring initial relaxation rates of inner (W_i) and outer (W_o, average value for left and right) lines of the $^{13}CH_2$ methylene group as defined by the following equations:

$$J_{CH}^*(\omega) = \frac{1}{4}\frac{r_{CH}^6}{h^2\gamma_H^2\gamma_C^2}(W_i + W_o) \quad (1a)$$

$$J_{HCH}(\omega_C) = \frac{5}{3}\frac{r_{CH}^6}{h^2\gamma_H^2\gamma_C^2}(W_o - W_i) \quad (1b)$$

where

$$J_{CH}^*(\omega) = \tfrac{3}{10}(\tfrac{1}{3}J_{CH}(\omega_H - \omega_C) + J_{CH}(\omega_C) + 2J_{CH}(\omega_H + \omega_C))$$

and r_{CH} is the internuclear distance between carbon and its bonded hydrogens; h is Plank's constant divided by 2π; and γ_C and γ_H are the magnetogyric ratios for carbon and hydrogen nuclei, respectively. Auto- and cross-correlation spectral densities $J_{CH}(\omega)$ and $J_{HCH}(\omega_C)$, respectively, can be defined as

$$J_{CH}(\omega) = 4\pi\int_0^\infty \langle Y_{20}(\theta_{CHi}(t))Y_{20}(\theta_{CHi}(0))\rangle\cos\omega t\,dt$$
$$J_{HCH}(\omega_C) = 4\pi\int_0^\infty \langle Y_{20}(\theta_{CHi}(t))Y_{20}(\theta_{CHj}(0))\rangle\cos\omega_C t\,dt \quad (2)$$

where θ_{CHi} and θ_{CHj} denote the angles between different methylene CH bonds and, for example, the direction of the static magnetic field. It should be noted that although Eq. 1b is always valid, Eq. 1a is valid only when contributions from the chemical shift anisotropy relaxation mechanism can be neglected. Dipolar chemical shift anisotropy cross-correlation does not contribute to $J^*_{CH}(\omega)$ and $J_{HCH}(\omega_C)$ when the average initial relaxation rate from both multiplet outer lines is used to calculate W_o (Bain and Lynden-Bell, 1975; Daragan and Mayo, 1993a; Gaisin et al., 1993).

For many rotational motion models, one can write a general equation for auto- and cross-correlation spectral densities, $J_{ab}(\omega)$ (Lipari and Szabo, 1982a, b; Kay and Torchia, 1991; Daragan & Mayo, 1993b, 1994) as

$$J_{ab}(\omega) = S^2_{ab}\frac{\tau_o}{1+(\omega\tau_o)^2} + (P_2(\cos\theta_{ab}) - S^2_{ab})\frac{\tau_i^*}{1+(\omega\tau_i^*)^2} \quad (3)$$

where θ_{ab} is the angle between vectors **a** and **b**. For the cross-correlation spectral density, **a** $\neq$ **b**. The second order Legendre polynomial, $P_2(x) = \frac{1}{2}(3x^2 - 1)$. For tetrahedral geometry of methylene group, $P_2(\cos\theta_{ab})$ equals $-\frac{1}{3}$. τ_o is the correlation time of overall tumbling with the correlation time for internal motions, τ_i, being given by

$$(\tau_i^*)^{-1} = (\tau_i)^{-1} + (\tau_o)^{-1}. \quad (4)$$

The order parameter S^2_{ab} is a function of both molecular motion and geometry. For the auto-correlation spectral density, i.e., **a** = **b**, S^2_{ab} is reduced to the well known Lipari-Szabo order parameter S^2 (Lipari and Szabo, 1982a, b).

London (1978) and Shekar and Easwaran (1982) have shown that proline ring puckering motions can be described by a two-state (A and B) jump model with life times τ_A and τ_B. To describe ^{13}C relaxation with this model, one should consider an axis of rotation for every ring carbon. For exo-endo interconversion of the C_γ carbon (see Fig. 1), $C_\beta H_2$ and $C_\delta H_2$ methylene group rotations can be considered to occur about the C_α-C_β and N-C_δ bonds, respectively, whereas $C_\gamma H_2$ methylene group rotation can be considered to occur about an axis perpendicular to the $HC_\gamma H$ plane (London, 1978). In

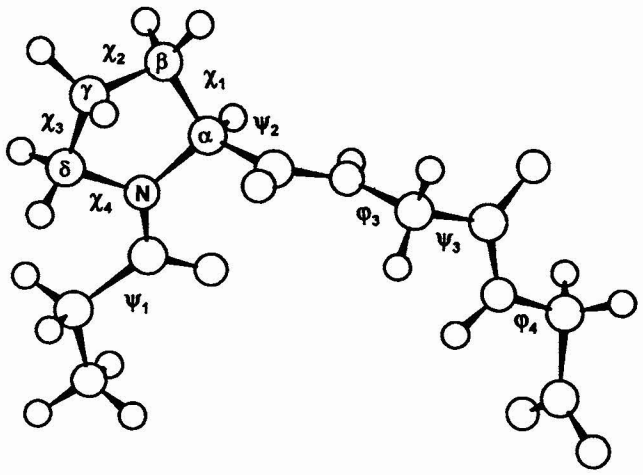

FIGURE 1 Structure of GPGG with dihedral angles labeled as discussed in the text.

a more general case, 2Δ can be used to denote the internal jump angle (jumps occur between $-\Delta$ and $+\Delta$, and values of Δ are different for various ring carbons) with an order parameter, S^2_{ab}, being written as (London, 1978; Daragan and Mayo, 1993a, b)

$$S^2_{ab} = P_2(\cos\theta_{ab}) - \frac{4\tau_A\tau_B}{(\tau_A+\tau_B)^2}\sin^2\Delta\,(a^1{}_{ab} + 4a^2{}_{ab}\cos^2\Delta) \tag{5}$$

where

$$\begin{aligned} a^1_{ab} &= 3\cos\theta_a\cos\theta_b\sin\theta_a\sin\theta_b\cos(\phi_a-\phi_b) \\ a^2_{ab} &= \tfrac{3}{4}\sin^2\theta_a\sin^2\theta_b\cos 2(\phi_a-\phi_b). \end{aligned} \tag{6}$$

The angles θ_a, ϕ_a, and θ_b, ϕ_b are the polar angles for vectors **a** and **b** in the molecular frame where the z axis is directed along the axis of internal rotation. For this model, the correlation time, τ_i, appeared in Eq. 4 can be written as

$$(\tau_i)^{-1} = (\tau_A)^{-1} + (\tau_B)^{-1}. \tag{7}$$

Assuming tetrahedral geometry for all proline methylene groups, endo $\leftrightarrow$ exo interconversion of C_γ can be expressed as

$$\theta_{C\beta H} = \theta_{C\delta H} = 70.5°;$$

$$\phi_{C\beta Hi} - \phi_{C\beta Hj} = \phi_{C\delta Hi} - \phi_{C\delta Hj} = 120°;$$

$$\theta_{C\gamma H} = 90°; \qquad \phi_{C\gamma Hi} - \phi_{C\gamma Hj} = 109.5°.$$

The angles for interconversion between two antisymmetric C_2 forms (London, 1978) are

$$\theta_{C\alpha H} = \theta_{C\delta H} = 70.5°; \quad \phi_{C\delta Hi} - \phi_{C\delta Hj} = 120°;$$

$$\theta_{C\beta H} = \theta_{C\gamma H} = 75.4°;$$

$$\phi_{C\beta Hi} - \phi_{C\beta Hj} = \phi_{C\gamma Hi} - \phi_{C\gamma Hj} = 115.1°.$$

The values for $\phi_{C\beta Hi} - \phi_{C\beta Hj}$ and $\phi_{C\gamma Hi} - \phi_{C\gamma Hj}$ were calculated by using Eq. 8:

$$\cos(\phi_a - \phi_b) = 1 - 4/(3\sin^2\theta_a), \tag{8}$$

which relates the difference between polar angles ϕ_a and ϕ_b with the angle between the direction of the internal rotation axis and vector **a** (or **b**) in case of $\theta_a = \theta_b$.

When $\omega\tau_o \ll 1$ (extreme narrowing condition), auto- and cross-correlation times can be expressed directly as

$$\tau_{ab} = J_{ab}(0) = S^2_{ab}\,\tau_o + (P_2(\cos\theta_{ab}) - S^2_{ab})\tau^*{}_i. \tag{9}$$

This is generally the case for the short peptides studied here. For the proline ring, one can determine four auto-correlation times τ_{CH} and three cross-correlation times τ_{HCH} from a ^{13}C-multiplet relaxation experiment. This is sufficient information to calculate rotational model parameters τ_o, τ_i, τ_A/τ_B, Δ_β, Δ_γ, and Δ_δ for one type of ring puckering process. Fig. 2 plots the dependence of the proline ring methylene group rotational auto- and cross-correlation times on the value of τ_A/τ_B. Unfortunately, neither auto- nor cross-correlation times are

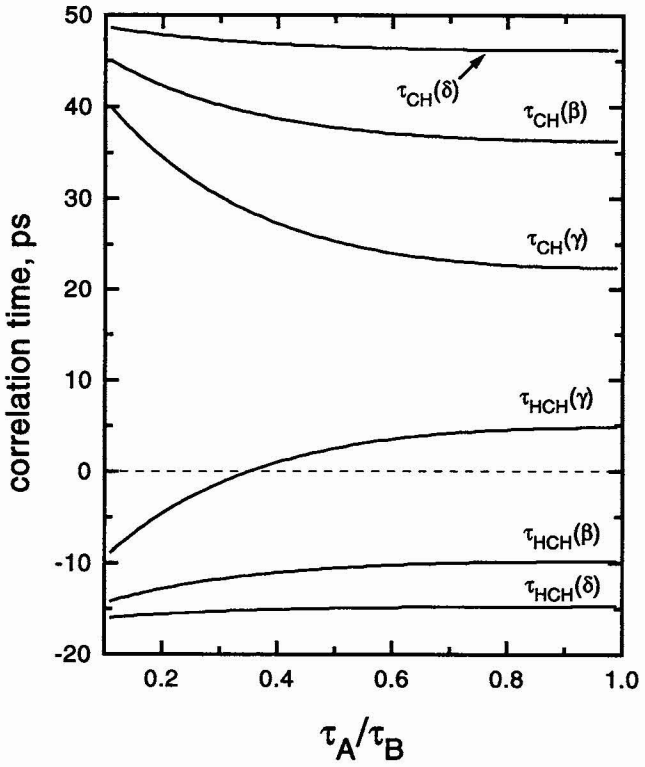

FIGURE 2 The dependence of auto- and cross-correlation times for proline carbons on the ratio of life times using the two-state jump model for endo-exo interconversion of the C_γ proline ring carbon. Parameters used are jump angles $\Delta_\beta = 20°$, $\Delta_\gamma = 30°$, and $\Delta_\delta = 10°$, and correlation times $\tau_o = 50$ ps and $\tau_i = 2$ ps (see text).

sensitive to the ratio τ_A/τ_B between 0.6 and 1.0 where the experimental data fall. Nevertheless, it is interesting to note that the cross-correlation time τ_{HCH} for C_γ is the most sensitive to τ_A/τ_B. This correlation time changes its sign when τ_A/τ_B becomes less than 0.35. These calculations were performed for the endo-exo interconversion of C_γ carbon for the angles $\Delta_\beta = 20°$, $\Delta_\gamma = 30°$, and $\Delta_\delta = 10°$ with $\tau_o = 50$ ps and $\tau_i = 2$ ps. Such insensitivity can also be observed in the dependence of correlation times on τ_i.

On the other hand, this type of analysis provides an opportunity to differentiate various rotational models in analyzing proline ring motional dynamics. To assess the sensitivity of relaxation parameters to various jump angles, the dependence of S^2_{ab} on the angle Δ is shown in Fig. 3. Similar calculations were also performed for proline C_γ endo-exo interconversion with $\tau_o = 50$ ps, $\tau_i = 2$ ps, and $\tau_A/\tau_B = 1$. The sensitivity of the cross-correlation order parameter to the angle Δ is readily apparent. For $\Delta = 25$–$35°$, S^2_{ab} even changed sign. This exemplifies the advantage of using cross-correlation times to study peptide internal motions.

MATERIALS AND METHODS

Peptides

Peptides PG, GP, and GPGG were purchased from Sigma Chemical Co. (St. Louis, MO) and were used without further purification. ^{13}C-enriched peptides GP, GPG, and PGG (enrichment in glycine positions) were synthesized

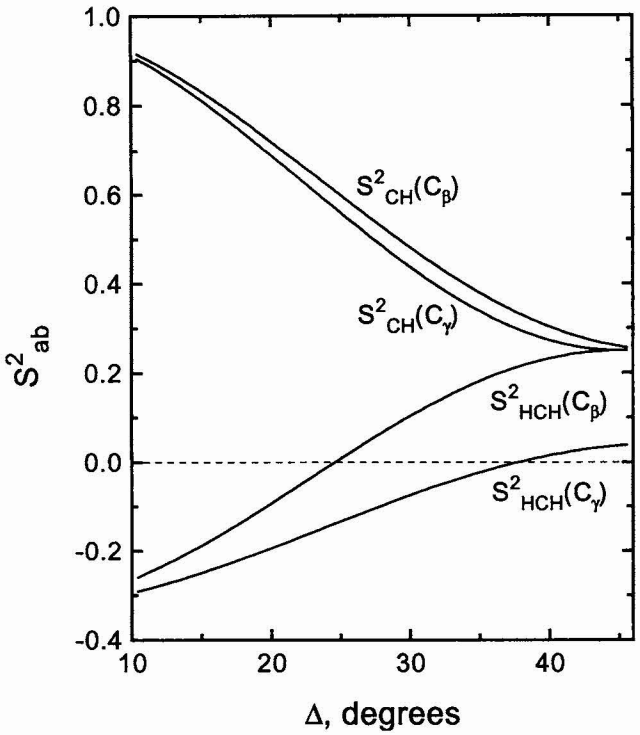

FIGURE 3 The dependence of auto- and cross-correlation order parameters for C_β and C_γ proline ring carbons on the jump angles for the two-state jump model. Calculations were made for the endo-exo interconversion of the proline ring C_γ carbon with correlation times τ_o = 50 ps and τ_i = 2 ps and for the ratio τ_A/τ_B = 1.

by using standard Fmoc-BOP solid-phase chemistry (Atherton and Sheppard, 1989). Details of the synthesis and purification are described in Daragan & Mayo (1993b). All samples were dissolved in D_2O, perdeuterated DMSO, or methanol in a 5-mm NMR tube. The pH of water solutions was adjusted by adding microliter quantities of NaOD or DCI.

NMR

^{13}C NMR measurements were performed on a Bruker AMX-500 or AMX-600 spectrometer at a ^{13}C frequency of 125 or 150 MHz, respectively. The temperature, varied from 278 to 343 K, was calibrated by measuring the proton chemical shifts of 1,2-dihydroxyethane. Spin-lattice relaxation was followed by using the inversion-recovery method with and without broadband proton decoupling. The number of acquisitions was varied from 32 to 4000 (for ^{13}C proton-coupled relaxation) to maintain a signal-to-noise ratio greater than 6. At least ten partially relaxed spectra were acquired for each relaxation experiment. To reduce errors from radio frequency field inhomogeneities, the composite 180° pulse ($90°_x$-$180°_y$-$90°_x$) was used. As discussed in Daragan et al. (1993), 90° pulses were calibrated by minimizing the signal after a 180° pulse and by checking for full inversion of resonances.

As relaxation curves were highly exponential, a relaxation delay of 5 × T_1 was generally used. Strong nonexponential behavior in relaxation curves is observed only when high rotational anisotropy is present, i.e., when cross-correlation spectral densities $J_{HCH}(\omega_o)$ are highly positive (Daragan et al., 1974). This is not the case for any of the peptides studied here. Some relaxation measurements with longer delays, however, were performed to verify this.

Auto-correlation (τ_{CH}) and cross-correlation (τ_{HCH}) times were calculated from initial relaxation rate curves by using Eq. 1. Considering the error in determining initial relaxation rates and cross-correlation terms, Daragan et al. (1993b) have calculated relaxation curves for ^{13}C NMR multiplet inner and outer lines as the ratio τ_o/τ_i (ratio of the overall and internal motional correlation times, respectively) is varied from 1 to 10 to 100. On a semilogarithmic scale, quasi-exponential behavior for all relaxation curves is observed. Daragan and Khazanovich (1979) have shown that, at the extreme narrowing limit (observed for all peptides in this study), one can obtain J_{HCH}, the dipolar cross-correlation spectral density, from the difference between initial relaxation rates of outer and inner lines with an error <2% with respect to W_{CH}. This is achieved by using the parabolic approximation to the initial slope of relaxation curves plotted on the semilogarithmic scale. To obtain accurate initial slopes from the parabolic approximation, at least 10 experimental points with a good decay profile are required. For relaxation data showing poorer statistics, it is preferable to approximate the decay curve with a single exponential. In this case, systematic errors are still less than 5% (Daragan et al., 1993b).

The main error in determining relaxation rates arises from data points at the tail end of the relaxation curve. One way to reduce this error is to calculate relaxation rates by using a weighted function like $A(t) = \exp(-2W_w t)$, where W_w is calculated by the least-squares method and then minimized according to the function

$$S = \Sigma \exp(-2W_w t_i)(I_o - I_i - A \exp(-Wt_i))^2 \quad (10)$$

where I_o and I_i are equilibrium and transient values of resonance line amplitudes. W_w can be calculated by minimizing the function $\Sigma(I_o - I_i - A \exp(-W_w t_i))^2$, and then, by using the determined value of W_w in Eq. 8, W can be calculated. All relaxation data in this paper have been calculated by using this method. Correlation coefficients from these fits were normally better than 0.98. In cases where T_1 values were measured two or three times, standard deviations were less than ~5%. Note also that $J_{HCH}(\omega_o)$ is determined from the difference of W_o and W_i. This significantly reduces systematic errors in determining $J_{HCH}(\omega_o)$.

Computer modeling

Molecular dynamics (MD) simulations were used to provide a more physically meaningful picture of the internal motions in the proline ring and internal rotations of glycine residues. All calculations were performed on a Silicon Graphics Challenge-L computer (4 R4400 CPUs) using the DISCOVER program (Version 3.1, Biosym Technologies) with standard AMBER potential energy parameters. Periodic boundary conditions were applied to a 20 × 20 × 20 Å^3 cell (cutoff distance of 10 Å) containing the peptide and 240 water molecules. Calculations were done on the zwitterionic form of the peptide so as to be more comparable with conditions used for the relaxation experiments. Simulations ran 10^6 steps with time incremented in units of 10^{-15} s. Molecular coordination files were recorded every 200 steps after stabilization of the total energy (~2.5 × 10^4 steps). Start files for molecular dynamics runs were the result of conjugate gradient minimizations of the peptide/water system. In cases for which individual runs were either repeated or compared in regards proline ring motions from one peptide to another, MD simulations were found to be reproducible.

RESULTS AND DISCUSSION

^{13}C NMR data

^{13}C resonance assignments were made by using proline and glycine $^{13}CH_2$ chemical shift data from Jardetsky and Roberts (1981). For dipeptides GP and PG, assignments were straightforward. For GPG, PGG, and GPGG, sequence-specific glycine resonance assignments were made by using the pH dependence of $^{13}CH_2$ chemical shifts (data not shown). For GPGG, NH_2 and COOH-terminal glycine (G1 and G4) $^{13}CH_2$ resonances are significantly shifted at high and low pH values, respectively, reflecting pK_as of the NH_2-terminal amine and COOH-terminal carboxylate groups. The G3 resonance remains mostly unshifted through the entire pH range. The zwitterionic form of GPGG exists between pH 5 and 7.

The following subsections present results on (1) *cis/trans*-proline isomer states, (2) proline ring puckering, (3) glycine backbone motions, and (4) effects from lower dielectric solvents DMSO and methanol. Whereas bond rotations in GPGG have been studied in detail, various other proline-containing glycine-based di- and tripeptides have been studied to simplify some analyses and calculations. Tables 1 and 2 are organized to provide an overview of experimental/theoretical data on proline and glycine methylene motional parameters, respectively.

Cis/trans-proline isomer states

For peptides containing a glycine NH_2-terminal to proline, two sets of resonances, one major (~70%) and one minor (~30%), were observed and were assigned to *trans*- and *cis*-proline states, respectively, based on their relative intensities and chemical shifts (Grathwohl and Wuthrich, 1981).

For the *trans*-proline isomer state, Fig. 4 plots proline ring ^{13}C relaxation curves, representative of typical data from which T_1 values have been derived. For *cis* and *trans* isomers of GP, Fig. 5 plots dipolar auto-correlation times, τ_{CH}, versus the inverse temperature in units of K^{-1}. For GP, as well as for other glycine-based proline-containing peptides studied, no significant differences in auto-correlation times and activation energies E_{CH} (Figs. 5, 6, and 7, Tables 1 and 2) for proline CH_2 groups in *cis* and *trans* states were found. For the NH_2-terminal glycine, however, slight differences in auto-correlation times mandated the use of ^{13}C-enriched glycine to increase experimental accuracy and ^{13}C multiplet spectroscopy to derive dipolar cross-correlation times, which are more sensitive to bond rotational anisotropy (Daragan and Mayo, 1992). Table 2 shows that cross-correlation times for G1 in the *trans* conformation are more negative than corresponding values for G1 in the *cis* state. This indicates relatively slower (more restricted) *trans* state G1 Ψ_1 bond rotations (Daragan and Mayo, 1993b). This conclusion is supported by Ψ_1-bond rotational energy profiles that were calculated for GP in both *trans* and *cis* states. Before these calculations, the conformation of GP was energy minimized by using the conjugate gradient method. As these energy profiles look essentially the same as those given for triglycine in Daragan and Mayo (1993b), these data are not shown here. In general, two minima are apparent for either the *trans* or *cis* state. The depth of the left minimum for the *cis* conformation is 0.5 kcal/mol less than that for *trans*. This indicates relatively greater Ψ_1-bond rotational freedom in the *cis* conformation and suggests that intramolecular interactions may be responsible for differences in relaxation behavior of *cis* and *trans* isomers.

MD calculations were also performed for both GP conformers in water ($20 \times 20 \times 20$ A^3 cell with periodic boundary conditions; pH 6; temperature, 303 K; length of MD run, 1000 ps) and in vacuo to study the influence of potential intermolecular solvent interactions on *cis* and *trans* isomer motional dynamics. The correlation functions, $\Phi_m(t) = \langle \cos(m(\Psi_1(t) - \Psi_1(0))) \rangle$, which are important in describing NMR relaxation parameters (Daragan and Mayo, 1993b), were calculated from $\Psi_1(t)$ trajectories. The limiting values of $\Phi_m(\infty)$ were estimated by using Eq. 11:

$$\Phi_m(\infty) = \langle \cos(m\Psi_1(t)) \rangle^2 + \langle \sin(m\Psi_1(t)) \rangle^2, \quad (11)$$

which was obtained from the well known property of

TABLE 1 Parameters of the proline ring puckering motions in PG, GP, and in GPGG in different solvents

Peptide + solvent	Atom	T_1	τ_o	τ_i	Δ	τ_A/τ_B	τ_{CH}	τ_{HCH}	$\tau_{CH}^{(exp)}$	$\tau_{HCH}^{(exp)}$	E_{CH}
GPGG + water	C_α	0.90	49.5	2.4		0.96	50		52 (2)		4.2 (0.2)
	C_β	0.60			20		37	−10	39 (1.5)	−4.2 (2.45)	4.3 (0.2)
	C_γ	0.87			26		28	0.6	27 (1.5)	−2 (2)	4.3 (0.2)
	C_δ	0.56			12		44	−14	42 (1.5)	−18 (4)	4.5 (0.2)
GPGG + DMSO	C_α	0.32	149	2.4		0.97	149		149 (8)		2.5 (0.2)
	C_β	0.27			27		84	−17	86 (5)	−12 (5)	1.9 (0.2)
	C_γ	0.35			45		65	16	68 (4)	21 (7)	2.1 (0.3)
	C_δ	0.21			16		123	−37	114 (7)	−50 (10)	2.4 (0.2)
GPGG + methanol	C_α	0.48	101	4.6		0.99	101		98 (4)		1.6 (0.15)
	C_β	0.43			28		54	−9	55 (3)	−4 (3)	1.7 (0.15)
	C_γ	0.55			33		40	14	43 (2)	18 (6)	1.7 (0.15)
	C_δ	0.33			22		70	−18	71 (3)	*	1.3 (0.15)
PG + water	C_α	1.96	23.9	1.9		0.94	24		24 (2)		
	C_β	1.68			31		12	−2	14 (2)	−1 (2)	
	C_γ	2.14			35		12	2	11 (2)	1 (2)	
	C_δ	1.68			28		14	−3	14 (2)	−2 (3)	
GP (*trans*) + water	C_α	1.38	34				34.3		34.3 (2)		4.4 (0.3)
	C_β	1.17			25.5		20.2	−4.5	20.2 (2)		4.6 (0.3)
	C_γ	1.29			26.2		18.2	1.1	18.2 (2)		5.0 (0.3)
	C_δ	0.92			19.2		25.5	−7.0	25.6 (2)		4.7 (0.3)
GP (*cis*) + water	C_α	1.42	33				33.4		33.4 (2)		4.8 (0.4)
	C_β	1.11			23.7		21.3	−5.1	21.3 (2)		5.3 (0.4)
	C_γ	1.18			24.0		19.8	−0.6	19.9 (2)		4.8 (0.4)
	C_δ	0.94			18.8		25.1	−7.0	25.0 (2)		4.6 (0.4)

All correlation times are in picoseconds; ^{13}C spin-lattice relaxation times with proton decoupling conditions are in seconds; Δ angles are in degrees; and activation energies are in kcal/mol. Experimental errors have been given in parentheses. All data are at 303 K. *Data are not available because of overlapping resonances. All motional parameters are given for the model of exo-endo interconversion of C_γ. For GP it was assumed that $\tau_i = 2$ ps and $\tau_A/\tau_B = 1.0$.

TABLE 2 Motional parameters for glycines in small proline-containing peptides in different solvents

Peptide + solvent	Glycine	T_1	τ_{CH}^{exp}	τ_{HCH}^{exp}	E_{CH}
GPGG + water	G1	0.54	44 (2)	−18 (6)	4.7 (0.2)
	G3	0.57	41 (2)	−6 (2)	4.7 (0.2)
	G4	0.91	26 (1)	2 (2)	4.7 (0.2)
GPGG + DMSO	G1	0.16	151 (6)	*	2.7 (0.15)
	G3	0.17	136 (5)	−48 (10)	2.3 (0.15)
	G4	0.20	118 (5)	−19 (6)	2.5 (0.15)
GPGG + methanol	G1	0.33	72 (3)	−23 (6)	1.5 (0.1)
	G3	0.32	73 (3)	−31 (8)	1.5 (0.1)
	G4	0.36	65 (3)	−10 (3)	1.6 (0.1)
PG + water	G2	1.21	19.5 (1)	−1.6 (0.5)	
GP (*trans*) + water	G1	0.87	27.0 (0.5)	−9.7 (3)	4.9 (0.3)
GP (*cis*) + water	G1	0.96	24.6 (1)	−7.0 (2)	4.6 (0.3)
GPG (*trans*) + water	G1	0.72	32.9 (1)		4.4 (0.1)
	G3	1.13	20.8 (0.5)		4.9 (0.3)
GPG (*cis*) + water	G1	0.72	32.8 (1)		4.4 (0.1)
	G3	1.05	22.5 (0.5)		4.9 (0.2)
PGG + water	G2	0.87	27.1 (1)	−0.2 (0.4)	
	G3	1.28	18.4 (0.5)	0.2 (0.4)	

All correlation times are given in picoseconds. Some typical ^{13}C spin-lattice relaxation times, T_1 (in seconds) are listed. Auto- and cross-correlation times shown were measured at 303 K. Activation energies are given in kcal/mol. Experimental errors are shown in parentheses for correlation times and activation energies. *This value could not be measured because resonance overlap.

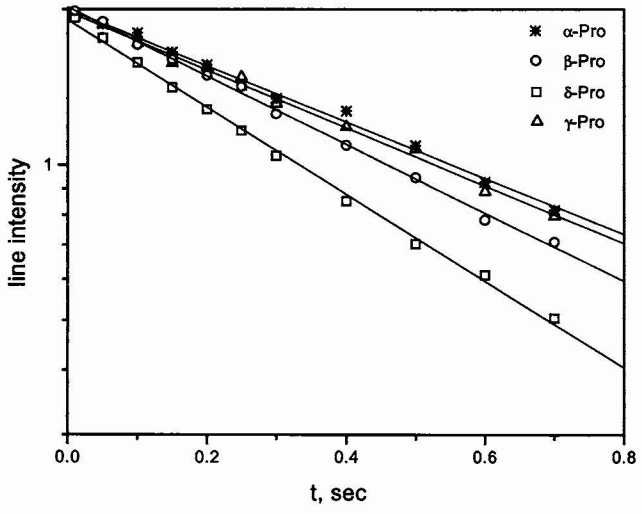

FIGURE 4 ^{13}C T_1 relaxation curves for all proline ring carbons in the dipeptide GP in water, pH 6, at 303 K. Symbols are identified in the figure.

correlation functions:

$$\lim_{t\to\infty} \langle A(0)B(t)\rangle = \langle A(t)\rangle\langle B(t)\rangle. \qquad (12)$$

The order parameters, S^2_{CH}, for glycine CH bond rotational motions were calculated from $\Phi_1(\infty)$ and $\Phi^2(\infty)$ by using Eqs. 26 and 29 of Daragan and Mayo (1993b). For tetrahedral geometry of the glycine methylene group, one can write

$$S^2_{CH} = \tfrac{1}{9} + \tfrac{8}{27}(\Phi_1(\infty) + 2\,\Phi_2(\infty)). \qquad (13)$$

In vacuo, S^2_{CH} is 0.53 and 0.49 for *trans* and *cis* states, respectively. In water, these values remain approximately the same.

To compare these calculated values with experimental ones, S^2_{CH} was estimated from the ratio $\tau_{CH}(G)/\tau_{CH}(P)$. For

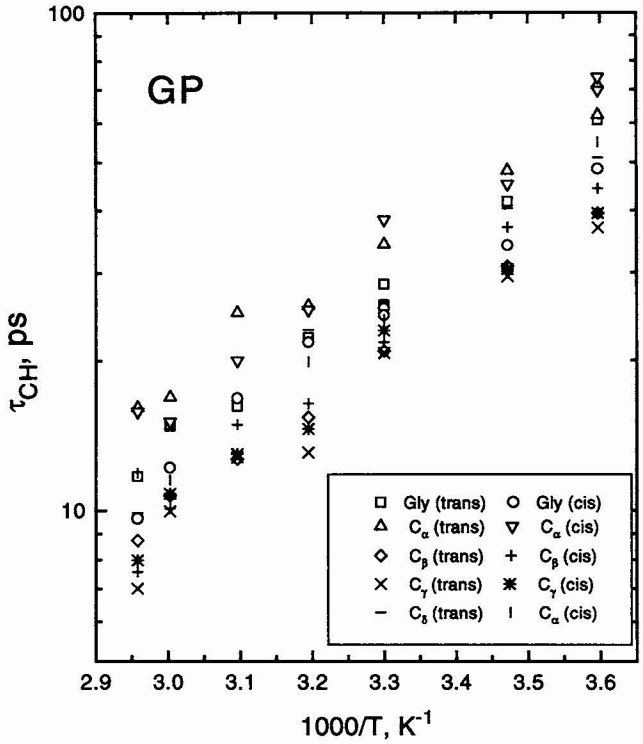

FIGURE 5 The temperature dependence of auto-correlation times, τ_{CH}, in GP in water at pH 6 for *trans* and *cis* peptide conformations.

both C_α atoms of glycine, S^2_{CH} is ~0.7, significantly larger than S^2_{CH} obtained from MD calculations. There are two reasons for this discrepancy. First, the correlation time for internal rotations, τ_i, in this short peptide may be comparable with the overall tumbling correlation time, τ_o. Second, recoil rotations (Daragan and Mayo, 1994) that effectively reduce the amplitude of restricted Ψ^1-bond rotations in the laboratory frame may be causal. To estimate the influence of τ_1/τ_o on S^2_{CH}, one can write Eq. 3 under extreme narrowing

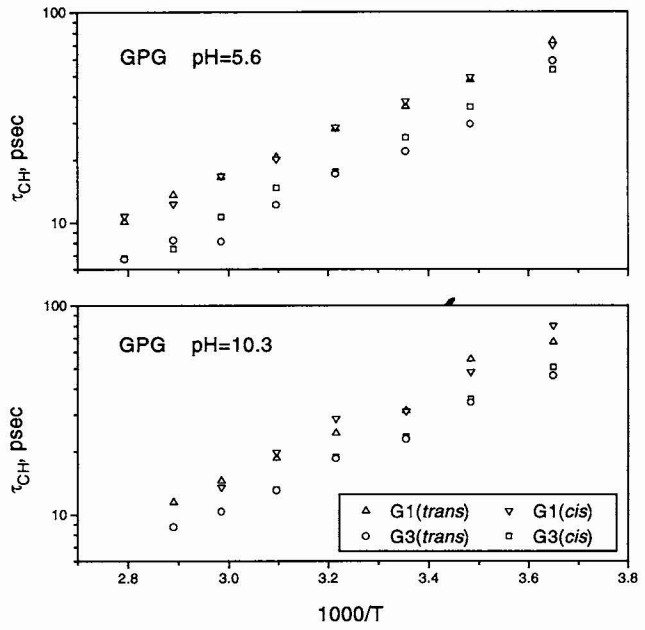

FIGURE 6 The temperature dependence of auto-correlation times, τ_{CH}, in GPG in water at pH 6 for *trans* and *cis* peptide conformations.

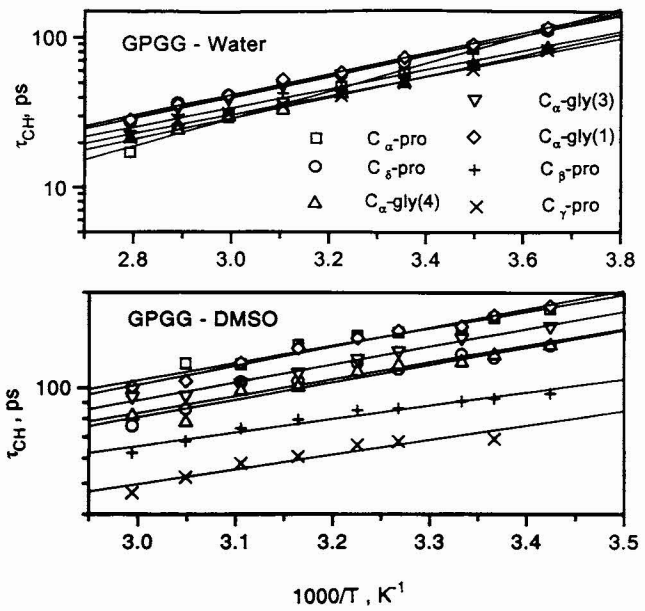

FIGURE 7 The temperature dependence of auto-correlation times, τ_{CH}, in GPGG in water (pH 6) and in DMSO.

conditions in the form:

$$S^2_{CH} = \tau_{CH}/\tau_o - \tau_i/\tau_o\,(1 - \tau_{CH}/\tau_o). \qquad (14)$$

Here, it is apparent that the actual value of S^2_{CH} is always less than that estimated from the ratio τ_{CH}/τ_o. However, even when $\tau_{CH}/\tau_o = 0.7$ and $\tau_i/\tau_o = 0.2$, for example, the error in estimating S^2_{CH} is only 0.06, which cannot explain the discrepancy between calculation and experiment. On the other hand, if Ψ_1 changes, for example, as the result of conformational jumps with angular difference $\Delta\Psi_1$, then proline in the laboratory frame will be rotated by an angle $\Delta\Psi_p$ and glycine will be rotated by an angle $\Delta\Psi_G$ in the opposite direction such that $|\Delta\Psi_p| + |\Delta\Psi_G| = |\Delta\Psi_1|$. The ratio $|\Delta\Psi_G|/|\Delta\Psi_1|$ will always be less than 1. Therefore, observable rotational jumps or fluctuation amplitudes will be effectively reduced. This ratio depends on various intramolecular interactions and on the ratio of the moments of inertia for proline and glycine residues with respect to the axes of Ψ_1-rotation (Daragan and Mayo, 1994). In GP, this recoil effect (Moro, 1987a,b) for Ψ_1-bond rotation is more pronounced than in GPGG where the moment of inertia of the PGG segment is much larger than that for the NH_2-terminal glycine residue alone. An in-depth analysis of this will not be considered here, but one should consider that such recoil effects may lead to larger order parameters.

Proline ring puckering

Correlation times of proline ring methylenes have many similar features. Table 1 summarizes experimental auto- and cross-correlation times, i.e., τ_{CH} and τ_{HCH}, respectively, for C_α, C_β, C_γ, and C_δ carbons in GPGG, PG, and GP. For each of these peptides, C_δ auto-correlation times are largest, whereas those of C_γ are smallest. More positive $C_\gamma H_2$ cross-correlation times indicate that the C_γ methylene group is relatively the most mobile within the proline ring. Activation energies, E_{CH}, (calculated from the temperature dependence of auto-correlation times) for proline ring carbons in GPGG, PG, and GP are nearly the same and are approximately equal to the pure water viscosity activation energy, $E_v = 4.6$ kcal/mol (Tyrrell, 1961) or to the activation energy for the self-diffusion of water, $E_D = 5.0$ kcal/mol (McCall et al., 1959). This underscores the importance of solvent-peptide interactions in modulating motional dynamics in these systems. Moreover, as E_{CH} for proline ring carbons in GPGG is less than that in GP and PG, it can be argued that proline ring puckering in a larger peptide is less influenced by solvent interactions than it is in a shorter peptide.

For insight into which proline ring puckering model is most applicable for NMR relaxation data analysis, MD calculations were performed on GPGG in water. Fig. 8 shows the time dependence of proline side-chain χ_1, χ_2, χ_3, and χ_4 dihedral angles. Strongly correlated χ_i angle jumps between two conformational states are observed. Amplitudes of χ_2 and χ_3 jumps are equal but rotate in opposite directions suggesting that an endo-exo interconversion mechanism in proline ring puckering motions can exist. χ_4 jump amplitudes are the smallest but are also strongly correlated with other χ_i angle jumps.

As MD simulations indicate the dominance of jumps between two states, a simple two-state jump model (Eq. 3–7) will be used to analyze experimental data and to describe proline ring puckering. With seven experimental parameters (four auto-correlation times, τ_{CH}, for C_α, C_β, C_γ, and C_δ carbons and three cross-correlation times, τ_{HCH}, for $C_\beta H_2$, $C_\gamma H_2$, and $C_\delta H_2$ methylene groups), one can determine six model parameters: τ_o, τ_i, τ_A/τ_B, Δ_β, Δ_γ, and Δ_δ. Table 1 gives these

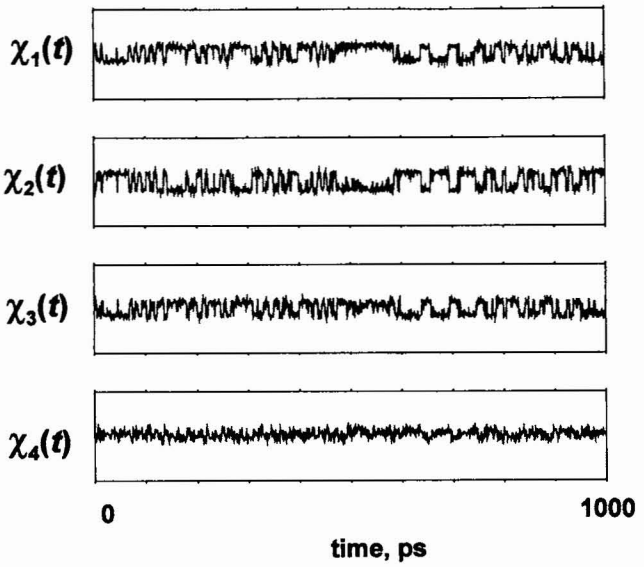

FIGURE 8 The time dependence of proline ring dihedral angles in GPGG taken from a MD simulation in water at 350 K. Calculations were performed in the $20 \times 20 \times 20$ A^3 cell with periodic boundary conditions. A 1000-ps run with sampling time 1 ps is shown. The *y* axes on each graph range from $-180°$ to 180°.

model parameters for GPGG and GP. Experimental correlation times are less sensitive to variations in the ratio τ_A/τ_B and correlation time τ_i than are other model parameters. Therefore, τ_i and τ_A/τ_B (Table 1) should be considered rough estimates. For GP, calculations were done for *trans* and cis conformations. Moreover, as multiplet relaxation in GP could not be done accurately due to overlapping *trans-cis* NMR lines, the minimization procedure used to derive model parameters considered only auto-correlation times. In this case, the values of $\tau_i = 2$ ps and $\tau_A/\tau_B = 1$ were fixed. All calculations shown in Table 1 were obtained for the model of the endo-exo interconversion of the C_γ carbon. Table 1 also gives the values of the correlation times τ_{CH} and τ_{HCH} recalculated with derived model parameters.

The values of Δ_β, Δ_γ, and Δ_δ for GPGG and GP in water are in good agreement with those values derived for poly-(Pro-Gly)^n and poly-(Pro[7]) (London, 1978), which indicates that proline ring puckering motions do not depend significantly on the size of the peptide. Δ_i angles in GPGG and in GP are nearly the same, whereas those in PG are slightly larger. Experimental and calculated correlation times agree within experimental error (shown in parentheses). Although the endo-exo interconversion model is capable of explaining both auto- and cross-correlation times, calculations were also made on GPGG by using the model of interconversion between two antisymmetric C_2 forms. This model also gave relatively good agreement between experimental and calculated auto- and cross-correlation times. Moreover, the values of Δ_i angles (data not shown) are close to those obtained from the endo-exo interconversion model, suggesting that both proline ring puckering mechanisms are possible in aqueous solution. As will be discussed later, this is not the case in lower dielectric solvents. In addition, Δ_i angles compare favorably with χ_i jump amplitudes taken from MD simulations. In general Δ_i and χ_i values vary at most by ~30%. For GPGG and GP, the temperature dependence of Δ_β, Δ_γ, and Δ_δ (data not shown) is rather flat, i.e., only approximately a 2–5° change on increasing the temperature by 60 K. This indicates that the enthalpic contribution to proline ring puckering is minimal at best.

Glycine backbone motions

For GPGG, PG, GP, GPG, and PGG, Table 2 lists experimental auto- and cross-correlation times and activation energies estimated from the temperature dependence of auto-correlation times. For the NH_2-terminal glycine, G1, the cross-correlation time, τ_{HCH}, is always negative. In GGG, τ_{HCH} for G1 is close to zero (Daragan and Mayo, 1993b). This indicates that G1 backbone motional restrictions are greater when a proline residue is on the COOH-terminal side. Auto- and cross-correlation times for COOH-terminal glycines in GPG and PG and for G3 in GPGG also indicate more restricted backbone motions for the residue on the COOH-terminal side of proline. The cross-correlation time, τ_{HCH}, for the glycine methylene group in PG, for example (see Table 2), is negative, whereas τ_{HCH} for G3 in GGG is slightly positive. Therefore, despite the relatively large three-bond separation of the glycine methylene from the proline ring, the influence of proline on its COOH-terminal neighbor is still significant and causes restricted internal rotations. This confirms the well known fact that proline acts as a good restrictor of protein backbone mobility. Insertion of one more glycine between proline and glycine on the COOH-terminal side (see data for PGG and GPGG, Table 2) practically removes the influence of proline on COOH-terminal glycine motions. The ratio of τ_{HCH}/τ_{CH} for G4 approaches that of G3 in GGG.

These experimental data are supported by φ- and Ψ-bond rotational energy profiles, which were calculated by using standard AMBER potential energy parameters in the DISCOVER program (Version 2.3.0, Biosym Technologies). The conformation of GPGG was first energy minimized by using the conjugate gradient method, which yielded the following equilibrium values for backbone dihedral angles: $\Psi_1 = -176.6°$, $\Psi_2 = 116.9°$, $\varphi_3 = 174.8°$, $\Psi_3 = -95.3°$, and $\Psi_4 = -178.3°$. These angles were taken as the conformation of lowest energy from which bond rotational energy profiles (Fig. 9) were calculated. On comparing $E(\Psi_1)$ in GPGG and in GGG (Daragan and Mayo, 1993b), it is apparent that in GGG this potential function has only two minima located at $\Psi_1 = -90°$ and $\Psi_1 = +90°$. In GPGG, a third minimum is observed at $\Psi_1 = 180°$, and the barrier height between minima at $\Psi_1 = 90°$ and $\Psi_1 = 180°$ is equal to 1.5 kcal/mol, which is 0.5 kcal/mol less than that between minima at $\Psi_1 = 90°$ and $\Psi_1 = -90°$ in GGG. Despite this, Ψ_1-bond rotations are faster in GGG than in GPGG as is evidenced by comparing respective G1 τ_{CH} values. In GGG, τ_{CH} for G1 is 20 ps at 303 K whereas in GPGG it is 33 ps. Moreover, in the short GP peptide, τ_{CH} for the terminal glycine is 25–27 ps. Interestingly, in GPGG, τ_{CH} for G3 is shorter

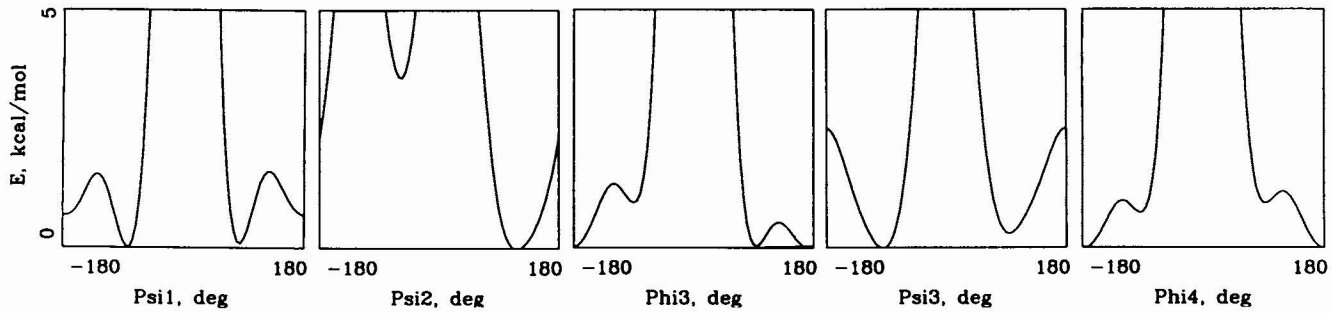

FIGURE 9 Bond rotational energy profiles for backbone dihedral angles in GPGG in vacuo calculated by using the DISCOVER program.

than it is for G1. Qualitatively, this indicates that G3 motions are determined by both Ψ_2 and φ_3 internal rotations with respect to the massive, more internally immobile proline residue. The Ψ_2-bond rotational energy profile (Fig. 9) has a relatively flat minimum allowing for rather large amplitude rotational fluctuations. The φ_3-bond rotational energy profile suggests the presence of jumps about the main minimum at $\varphi_3 = 180°$.

MD calculations shown in Fig. 10 exemplify backbone φ and Ψ dihedral angle time dependencies for GPGG in water. To compare the characteristics of φ,Ψ-bond rotations in GPGG and GGG, MD calculations were performed for GGG in water under the same conditions of T = 350 K with periodic boundary conditions for a cube with dimensions 19 × 19 × 19 A^3. Calculated values of Φ_m are 0.085 (m = 1) and 0.24 (m = 2) for GGG and 0.14 (m = 1) and 0.45 (m = 2) for GPGG. Larger values of Φ_m effectively relate to more restricted Ψ_1 rotations in GPGG.

S^2_{CH}, calculated by using Eq. 12, is equal to 0.28 and 0.42 for G1 in GGG and GPGG, respectively. To estimate the values of S^2_{CH} from experiment by using Eq. 13, the overall tumbling correlation time, τ_o, was taken as the value of τ_o for G2 in GGG (Daragan and Mayo, 1993b) and of τ_{CH} for the proline ring α-carbon in GPGG. To a first approximation, one can assume that internal rotational correlation times are much less than τ_o. In this case, one can write from Eq. 3 that $S^2_{CH} = \tau_{CH}/\tau_o$. By using data from Table 2 in this paper and from Table 1 in Daragan and Mayo (1993b), one can obtain S^2_{CH} values that are equal to 0.25 and 0.43 for G1 in GGG and GPGG, respectively. These are in excellent agreement with data derived from MD simulations.

The effect of the ionization state of NH_2 and COOH termini was also investigated by deriving auto- and cross-correlation times for GPG and GP at pH 10 and 2. Results are essentially the same as those found for triglycine (Daragan and Mayo, 1993b); therefore, these data are not shown. The general conclusion is that deprotonation of either terminus leads to increased mobility of the respective terminal residue. This effect is most likely associated by a change in the potential number of peptide-water hydrogen bonds that can form when a proton is removed.

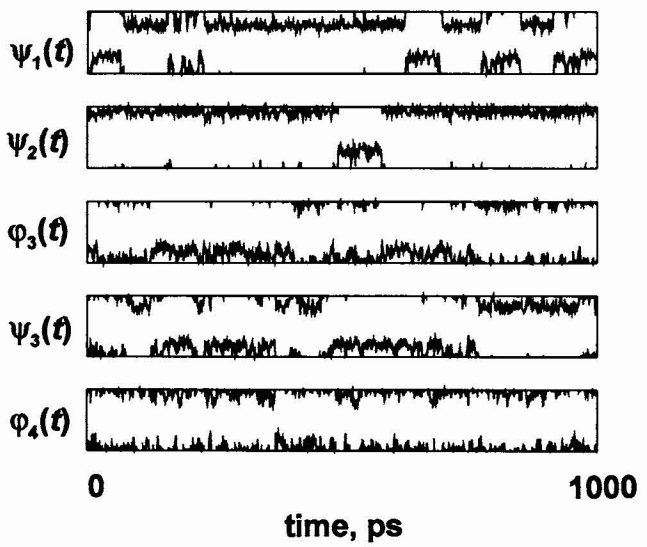

FIGURE 10 The time dependence of backbone dihedral angles in GPGG taken from a MD simulation in water as described in the legend to Fig. 8. The y axes on each graph vary from −180° to 180°.

DMSO and methanol solvent effects

Tables 1 and 2 show auto- and cross-correlation times for GPGG in two relatively low dielectric solvents, DMSO and methanol. Contrary to what was observed for proline ring puckering in water, the C_2 interconversion model cannot explain cross-correlation times, τ_{HCH}, for the $C_\gamma H_2$ methylene group when GPGG is in DMSO or methanol. The best fit of τ_{HCH} is 6.7 ps and 5.8 ps for DMSO and methanol, respectively. The experimental values of these cross-correlation times are 21 ps (DMSO) and 18 ps (methanol), which indicate that proline ring puckering by endo-exo interconversion is preferable in these lower dielectric solvents. Furthermore, Δ_i values for GPGG in DMSO and in methanol are larger than they are in water. The reason(s) for these differences are related to peptide-peptide and/or peptide-solvent interactions.

The temperature dependence of auto-correlation times, τ_{CH}, in water, DMSO, and methanol has been measured to further study the influence of solvent on proline ring puckering and peptide backbone dynamics. Fig. 7 shows some typical results for GPGG in water and DMSO, and Tables 1 and 2 give derived activation energies, E_{CH}, for all GPGG in water, DMSO, and methanol. It is interesting to note that in

TABLE 3 Auto-correlation times for GPGG carbons in methanol and DMSO at two concentrations

	G1	Pα	Pβ	Pγ	Pδ	G3	G4
Methanol							
40 mg/mL	73*	101	59	51	*	91	75
8 mg/mL	56	64	40	32	*	57	47
DMSO							
50 mg/mL	*	220	121	82	134	187	166
10 mg/mL	*	190	111	75	95	150	131

All correlation times are given in picoseconds. *Value could not be determined because of spectral overlap.

water and in DMSO, τ_{CH} for G3 is less than it is for G1 despite the fact that G3 is in the middle of the peptide. In methanol, these correlation times are approximately equal. E_{CH} in DMSO and methanol is considerably less than it is for activation energy due to solvent viscosity, E_v, which is equal to 3.8 and 2.3 kcal/mol for DMSO and methanol, respectively. This suggests that peptide-solvent interactions are less than solvent-solvent interactions.

To estimate the influence of different solvents on overall tumbling of GPGG, τ_{CH} for C_α proline ring carbons (which approximates the correlation time of overall tumbling τ_o) was compared with solvent viscosities, η. In classical hydrodynamic theory, τ_o is proportional to η. As viscosities for water, DMSO, and methanol at 303 K are 0.798, 1.85, and 0.51 cp (McCall et al., 1959; Tyrrell, 1961), respectively, the ratios of τ_o/η are equal to 64, 80, and 192 ps/cp in these solvents. The large value of this ratio in methanol suggests that considerable peptide aggregation is occurring. This effectively increases the relative value of the overall tumbling correlation time. Precipitation of GPGG in methanol at high temperatures supports this conclusion. In DMSO, some aggregation may be occurring, but this is minimal. For G3 and G4, the ratios τ_{HCH}/τ_{CH} can be estimated from data presented in Table 2. In DMSO and in methanol, these ratio are more negative than in water, suggesting more restricted backbone motions. This is consistent with the presence of peptide-peptide associations occurring in these lower dielectric solvents.

Comparison of auto-correlation times for GPGG in DMSO and in methanol at relatively high (40–50 mg/mL) and low (8 mg/mL) peptide concentrations is shown in Table 3. In general, auto-correlation time changes in either DMSO or in methanol are nearly the same for all carbons throughout the entire peptide. In methanol, peptide concentration has a greater effect on the correlation time (~40%) than in DMSO (10–20%). This supports the conclusion made above that intermolecular associations are greater in methanol than in DMSO. The nature of these associations is unknown. In DMSO, it is possible that one or two DMSO molecules could interact with one GPGG molecule to account for the observed changes in auto-correlation times. On the other hand, peptide-peptide interactions could be occurring.

CONCLUSIONS

Several general conclusions may be made regarding the role of proline in modulating peptide dynamics: (1) proline restricts ϕ,Ψ bond rotations $(i,i+1)$ and $(i,i-1)$ positions; (2) motions of NH_2-terminal residues are more restricted in the *trans*-proline state; (3) within the proline ring, the C_γ methylene is least restricted; (4) proline ring puckering in water occurs both via endo-exo and C_2 interconversions; whereas (5) in lower dielectric solvents the endo-exo mechanism is favored. Although normally used auto-correlations are useful in analyzing rotational motions, cross-correlation times are considerably more sensitive to differences in rotational anisotropy and allow better discrimination of various motional models.

This research was supported by National Science Foundation grant MCB-9420203.

We are grateful to Marek Kloczewiak for the synthesis of peptides GP, PG, and GPG.

NMR experiments were performed at the University of Minnesota High Field-NMR Laboratory.

REFERENCES

Atherton, E., and R. C. Sheppard. 1989. Solid Phase Peptide Synthesis: A Practical Approach. IRL Press, Oxford, UK.

Bain, A. D., and R. M. Lynden-Bell. 1975. The relaxation matrices for AX_2 and AX_3 nuclear spin systems. *Mol. Phys.* 30:325–356.

Clore, M., and A. Gronenborn. 1993. NMR of Proteins. CRC Press, Boca Raton, FL.

Daragan, V. A., T. N. Khazanovich, and A. U. Stepanyants. 1974. Cross-correlation effects of multiplet spectra of ^{13}C. *Chem. Phys. Lett.* 26:89–92.

Daragan, V. A., and T. N. Khazanovich. 1979. Study of molecular motion in liquids by the multiplet effect in spin-lattice relaxation. *In* Magnetic Resonance and Related Phenomena. Springer-Verlag, Heidelberg, Germany. 475.

Daragan, V. A., and K. H. Mayo. 1992. ^{13}C - {^1H} NMR/NOE and multiplet relaxation data in modeling protein dynamics of a collagen ^{13}C enriched glycine GXX repeat motif heptadecapeptide. *J. Am. Chem. Soc.* 114: 4326–4331.

Daragan, V. A., and K. H. Mayo. 1993a. Asymmetric ^{13}C NMR multiplet relaxation and dipolar-CSA cross-correlation for glycine C_α methylenes in peptides. *Chem. Phys. Lett.* 206:393–400.

Daragan, V. A., and K. H. Mayo. 1993b. Tri- and di-glycine backbone rotational dynamics investigated by ^{13}C NMR multiplet relaxation and molecular dynamics simulations. 1993. *Biochemistry.* 32: 11488–11499.

Daragan, V. A., and K. H. Mayo. 1994. Peptide dynamics in triglycine: coupling of internal bond rotations and overall molecular tumbling. *J. Phys. Chem.* 98:10949–10956.

Gaisin, N. K., I. R. Manyrov, and K. M. Enikeev. 1993. Cross-correlation effects in the spin-lattice relaxation of ethanol methylene ^{13}C. *Mol. Phys.* 80:1047–1057.

Grant, D. M., C. L. Mayne, F. Liu, and T.-X. Xiang. 1991. Spin-lattice relaxation of coupled nuclear spins with applications to molecular motion in liquids. *Chem. Rev.* 91:1591–1624.

Grathwohl, C., and K. Wuthrich. 1981. NMR studies of the rates of proline *cis-trans* isomerization in oligopeptides. *Biopolymers.* 20:2623–2633.

Jaenicke, R. 1991. Protein folding. *Biochemistry.* 30:3147–3161.

Jardetzky, O., and G. C. K. Roberts. 1981. NMR in Molecular Biology. Academic Press, New York.

Kay, L. E., and D. A. Torchia. 1991. The effects of dipolar cross-correlation on ^{13}C methyl-carbon T_1, T_2 and NOE measurements in macromolecules. *J. Magn. Resonance.* 95:536–547.

Lipari, G., and A. Szabo. 1982a. Model-free approach to the interpretation of NMR relaxation in macromolecules. I. Theory and range of validity. *J. Am. Chem. Soc.* 104:4546–4559.

Lipari, G., and A. Szabo. 1982b. Model-free approach to the interpretation of NMR relaxation in macromolecules. II. Analysis of experimental results. *J. Am. Chem. Soc.* 104:4559–4570.

London, R. E. 1978. On the interpretation of ^{13}C spin-lattice relaxation resulting from ring puckering in proline. *J. Am. Chem. Soc.* 100: 2678–2685.

McCall, W., D. C. Douglass, and E. W. Anderson. 1959. Diffusion in liquids. *J. Chem. Phys.* 31:1555–1557.

Moro, G. 1987a. Coupling of the overall molecular motion with the conformational transitions. I. The model system of the two coupled rotors. *Chem. Phys.* 118:167–180.

Moro, G. 1987b. Coupling of the overall molecular motion with the conformational transitions. II. The full rotational problem. *Chem. Phys.* 118: 181–197.

Shekar, S. C., and K. R. K. Easwaran. 1982. Proline ring conformations corresponding to a bistable jump model from ^{13}C spin-lattice relaxation times. *Biopolymers.* 21:1479–1487.

Tyrrell, H. J. V. 1961. Diffusion and Heat Flow in Liquids. Butterworths, London.

Werbelow, L. G., and D. M. Grant. 1977. Intramolecular dipolar relaxation in multispin systems. *Adv. Magn. Resonance.* 9:189–299.